

DOE/BC/14882--11

++ 16

1/1  
L. MCT

Quarterly Technical  
Progress Report  
for

**Responsive Copolymers for Enhanced  
Petroleum Recovery**

DE-AC22-92BC 14882

by

Charles McCormick  
Roger Hester

Department of Polymer Science  
University of Southern Mississippi  
Hattiesburg, MS 39406

**DISCLAIMER**

This report was prepared as an account of work sponsored by an agency of the United States Government. Neither the United States Government nor any agency thereof, nor any of their employees, makes any warranty, express or implied, or assumes any legal liability or responsibility for the accuracy, completeness, or usefulness of any information, apparatus, product, or process disclosed, or represents that its use would not infringe privately owned rights. Reference herein to any specific commercial product, process, or service by trade name, trademark, manufacturer, or otherwise does not necessarily constitute or imply its endorsement, recommendation, or favoring by the United States Government or any agency thereof. The views and opinions of authors expressed herein do not necessarily state or reflect those of the United States Government or any agency thereof.

Contract Begin Date September 22, 1992  
Contract Second Year End Date September 21, 1995

Current Year DOE Award \$276,650

Contracting Officer's Representative Jerry F. Casteel

for the time period of  
September 22, 1994 - December 22, 1994

ACQUISITION & ASSISTANCE DIV.

95 JAN 27 AM 10:58

RECEIVED  
USDOE/PETC

OK

**MASTER**

## **DISCLAIMER**

**This report was prepared as an account of work sponsored by an agency of the United States Government. Neither the United States Government nor any agency Thereof, nor any of their employees, makes any warranty, express or implied, or assumes any legal liability or responsibility for the accuracy, completeness, or usefulness of any information, apparatus, product, or process disclosed, or represents that its use would not infringe privately owned rights. Reference herein to any specific commercial product, process, or service by trade name, trademark, manufacturer, or otherwise does not necessarily constitute or imply its endorsement, recommendation, or favoring by the United States Government or any agency thereof. The views and opinions of authors expressed herein do not necessarily state or reflect those of the United States Government or any agency thereof.**

## **DISCLAIMER**

**Portions of this document may be illegible in electronic image products. Images are produced from the best available original document.**

---

## A. Task 1. Quaternary Ammonium Cyclopolymer Synthesis

Cationic quaternary ammonium polyelectrolytes have been the subject of increased research efforts in recent years due to their diverse commercial applications.<sup>1</sup> Among the most prominent technological water-soluble cationic ammonium polymers is poly(diallyldimethylammonium chloride), PDADMAC. Butler and Ingley<sup>2</sup> first reported the free radical polymerization of diallyldimethylammonium bromide yielding a water-soluble polymer. Later, Butler and coworkers<sup>3,4</sup> proposed and confirmed the formation of a linear cyclopolymer via intra-intermolecular polymerization, now termed cyclopolymerization. Although six-member rings are thermodynamically more stable, <sup>13</sup>C NMR studies<sup>5,6</sup> indicated that five-membered rings are predominant in PDADMAC for kinetic reasons.

Reported herein is the synthesis and solution properties of cyclocopolymers of diallylalkoxybenzylmethylammonium chloride and diallyldimethylammonium chloride.<sup>7</sup> The formation of ring structures along the polymer backbone is expected to increase the rigidity of the polymer chains in comparison to previously studied acrylamide copolymers.<sup>8</sup> Here we examine whether the distribution of the hydrophobic groups has a similar effect on the association properties. The introduction of phenyl groups allows precise determination of copolymer composition by UV spectroscopy.<sup>9,10</sup> Effects of hydrophobe length and concentration, electrolytes, surfactants and shear stress are studied by viscometric and photophysical measurements.

### Materials

All chemicals and reagent-grade solvents were purchased commercially and used as received. The deionized water used in the studies had a resistance of 18 M $\Omega$  and a surface tension of 70.8 mN m<sup>-1</sup>.

### Monomer Synthesis and Copolymerization

The synthesis of the hydrophobic comonomer N,N-diallyl-N-(4-alkoxybenzyl)-N-methylammonium chloride<sup>7</sup> is depicted in scheme 1. Diallylmethylamine was added to the 4-alkoxybenzyl chloride at 0 °C in a round-bottomed flask under a nitrogen atmosphere. The

solution was stirred at room temperature for two days to give a slightly yellow gel. Precipitation into ether gave a hygroscopic white solid in quantitative yield. Purity was confirmed via HPLC,  $^{13}\text{C}$  and  $^1\text{H}$  NMR.

Synthesis of the cyclocopolymer from N,N-diallyl-N,N-dimethylammonium chloride and N,N-diallyl-N-methyl-N-(4-alkoxybenzyl)ammonium chloride is illustrated in Scheme 2. To a 250 ml of 3-neck round-bottomed flask equipped with a mechanical stirrer, a nitrogen inlet and an outlet were added 60 ml of 60 wt% DADMAC aqueous solution and a desired amount of 50 wt% aqueous solution and hydrophobic comonomer. The solution was purged with nitrogen for one hour at 50 °C. A solution of potassium persulfate was introduced through a syringe. The total monomer to initiator molar ratio used in this study was kept constant at 500. The copolymer was precipitated into an ethanol-acetone mixture and dried under vacuum. Purification of the copolymer was performed by redissolving the sample in water and dialyzing against water using a membrane with 12,000-14,000 molecular weight cut-off. The polymer was recovered by freeze drying.

#### **A. Task 2. Characterization of Molecular Structure and Solution Behavior**

$^1\text{H}$  and  $^{13}\text{C}$  NMR spectra were recorded using a Bruker AC-200. A Mattson 2020 Galaxy Series FTIR was used to obtain infrared spectra. Purity of liquid samples was determined by GC utilizing a Hewlett Packard 5890 Series II Gas Chromatograph equipped with an Alltech AT-5 capillary column. A Hewlett Packard Model 1050 HPLC was used to determine the purity of solid samples. A Waters Bondapak C18 column was employed with methanol as the mobile phase. Classical light scattering studies were performed with a Chromatix KMX-6 low-angle laser light scattering spectrophotometer with a 2 mW He-Ne laser operating at 633 nm. Refractive index increments ( $dn/dc$ ) were obtained using a Chromatix KMX-16 differential refractometer. The molecular weight of poly (DADMAC) was measured in 0.5 M NaCl solution. For hydrophobically modified copolymers, methanol was used as a solvent in the light scattering studies to disrupt hydrophobic associations and to keep the copolymers from interacting with the filter. Steady-state fluorescence measurements were made with a Spex Fluorolog-2 fluorescence

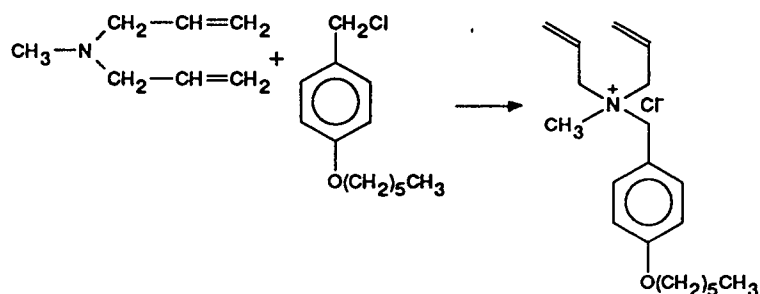
spectrometer and corrected for the wavelength dependence of the detector using an internal correction function provided by the manufacturer. Viscosity measurements were conducted with a Contraves LS-30 low shear rheometer at a constant shear rate of  $1.28 \text{ sec}^{-1}$  at  $25 \text{ }^\circ\text{C}$ , unless otherwise noted.

In order to assess the effects of hydrophobic monomer concentration on the copolymer conformation in deionized water, intrinsic viscosity was first determined utilizing the Fuoss relationship.<sup>11</sup> The viscometric studies were performed at low shear rate ( $1.28 \text{ sec}^{-1}$ ) to minimize shear-dependent conformational changes. Figure 1 shows the change of intrinsic viscosity as a function of hydrophobic group content for the hexyl- and octylbenzyl copolymer series. Intrinsic viscosities decrease continuously with increasing hydrophobe concentration for both hexyl and octyl copolymers. Similar behavior has been observed for hydrophobically modified poly(4-vinylpyridine)s.<sup>12-14</sup> These data imply that these copolymers form mainly intramolecular hydrophobic associations. This is consistent with previous studies indicating that random copolymers have a tendency toward intramolecular association in dilute solutions.<sup>8</sup> The decrease in the intrinsic viscosity for hexyl- and octyl-modified copolymer with increasing hydrophobic content reflects the increasing compactness of these amphiphilic systems in aqueous media.

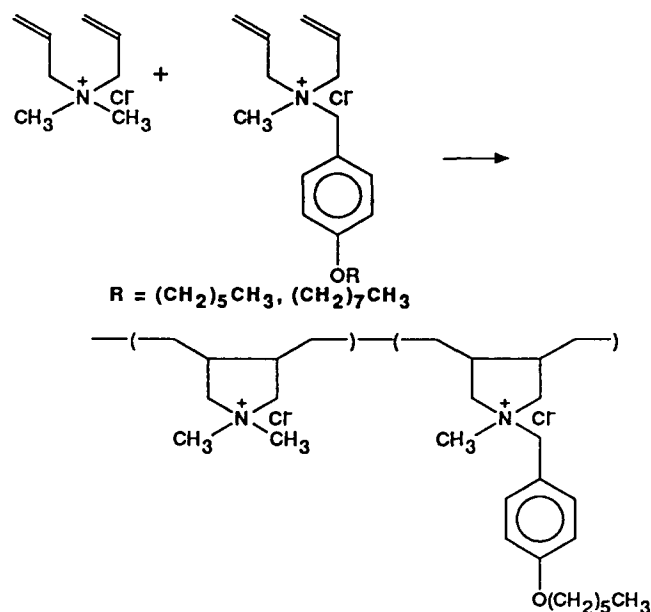
## References

1. *Chemical Economics Handbook*; Stanford Research Institute: Menlo Park, CA, 1983. pp. 581-1011I, pp. 581-2022L, pp. 581-1012D.
2. Butler, G.B.; Ingley, F.L.; *J. Am. Chem. Soc.* **1951**, *73*, 895.
3. Butler, G.B.; Angelo, R.J. *J. Am. Chem. Soc.* **1957**, *79*, 3128.
4. Butler, G.B. *Acc. Chem. Res.* **1982**, *15*, 370.
5. Johns, S.R.; Willing, R.I.; Middleton, S.; Ong, A.K. *J. Macromol. Sci., Chem.* **1976**, *A10*, 875.
6. Lancaster, J.; Baccei, L.; Panzer, H. *J. Polym. Sci., Polym. Lett. Edn.* **1976**, *14*, 549.
7. Chang, Y.; McCormick, C.L. *Polymer* **1994**, *35*, 3503.
8. Chang, Y.; McCormick, C.L. *Macromolecules* **1993**, *26*, 6121. Chang, Y.; Lochhead, R.Y.; McCormick, C.L. *Macromolecules* **1994**, *27*, 2145.
9. Valint, Jr., P.L.; Bock, J.; Schulz, D.N. in *Polymers in Aqueous Media*; J.E. Glass, Ed.; Advances in Chemistry Series No. 223; American Chemical Society: Washington, D.C., 1991. p. 399.

10. McCormick, C.L.; Middleton, J.C.; Grady, C.E. *Polymer* **1992**, *33*, 4184.
11. Fuoss, R.M.; Cathers, G.I. *J. Polym. Sci.* **1949**, *4*, 96.
12. Strauss, U.P.; Gershfeld, N.L. *J. Phys. Chem.* **1954**, *58*, 747.
13. Strauss, U.P.; Gershfeld, N.L.; Cook, E.H. *J. Phys. Chem.* **1956**, *60*, 577.
14. Ghesquiere, D.; Chachaty, C.; Ban, B; Locheux, C. *Makromol. Chem.* **1976**, *177*, 1601.



**Scheme 1.** Synthesis of N,N-diallyl-N-(4-hexyloxybenzyl)-N-methyl-ammonium chloride.



**Scheme 2.** Copolymerization of diallyl monomers to give hydrophobically modified cyclopolymers.

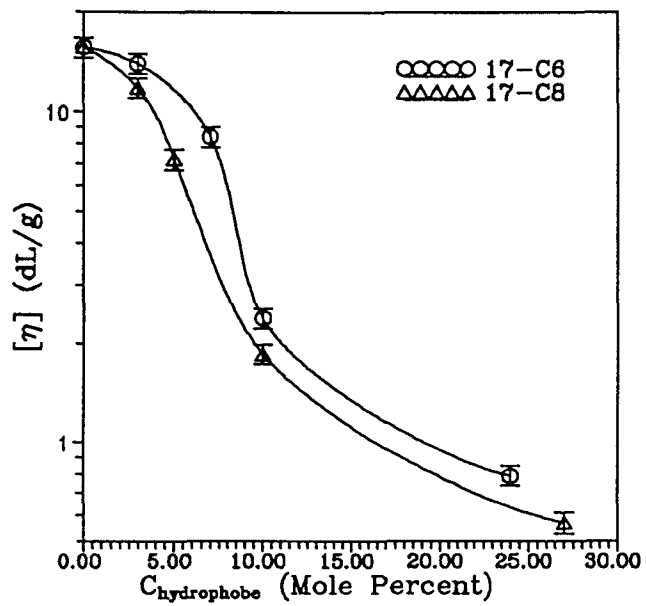


**Figure 1.** Effect of hexyl and octyl group content on the intrinsic viscosity  $[\eta]$  of hydrophobically modified cyclopolymers in deionized water at 25 °C.

## B. Task 1. $^{23}\text{Na}$ NMR Studies of Ion-Binding to anionic Polyelectrolytes

The behavior of uncharged polymers and polyelectrolytes in the presence of simple electrolytes is a subject of continuing research in our laboratory. The large viscosity losses and, ultimately, phase separation of anionic polyelectrolytes by a divalent cation are due to the strong chelating effect that reduces hydrodynamic volume and solvation. Sufficient inter- and intramolecular binding occurs to reduce the hydration of the polymer to a critical point at which phase separation occurs. The maintenance of viscosity in high concentrations of electrolytes is critical for application of polymers in areas such as enhanced oil recovery, drag reduction, and controlled release. Synthetic efforts have resulted in polymer systems that maintain viscosity in the presence of both monovalent and divalent ions and do not phase separate readily.<sup>1-5</sup> An increased understanding of the ion-binding and phase separation phenomena of these polymers is necessary for tailoring polymer systems for use in areas where high salt concentrations adversely affect performance.

The viscosity behavior and phase stability of polyelectrolytes in the presence of excess salts have been extensively studied.<sup>1-14</sup> Poly(acrylates)<sup>6-8</sup> and hydrolyzed polyacrylamide (HPAM)<sup>1,9-11</sup> exhibit large viscosity losses and may phase separate in the presence of divalent counterions such as  $\text{Mg}^{++}$ ,  $\text{Ca}^{++}$ , and  $\text{Ba}^{++}$ . Poly(sodium acrylate) (NaAA) precipitates from solution when the concentration of divalent counterion ( $\text{Mg}^{++}$ ,  $\text{Ca}^{++}$ ,  $\text{Ba}^{++}$ ) reaches a critical value relative to the number of anionic sites available (approximately 0.8 on an equivalent basis).<sup>6</sup> Macroscopic solution properties (viscosity, phase separation) of poly(vinylsulfonate) (PVS) are dependent on the nature of the counterion species.<sup>13,14</sup>

Copolymers of acrylamide with sodium 2-acrylamido-2-propanesulfonate (NaAMPS)<sup>1,3,4</sup> and 3-acrylamido-3-methylbutanoic acid (NaAMB) maintain viscosity in high concentrations of divalent salts and do not phase separate in the presence of  $\text{Ca}^{++}$  at temperatures up to  $100^\circ\text{C}$  (polymer structures are shown in Figure 1).<sup>3,4</sup> However, unlike NaAMPS, the NaAMB homopolymer will phase separate at temperatures above  $70^\circ\text{C}$  in high concentrations of  $\text{CaCl}_2$ .<sup>3</sup> The amount of  $\text{Ca}^{++}$  necessary to precipitate NaAMB far exceeds the stoichiometric

concentration required to bind to all of the anionic sites. This difference has been attributed to a weaker binding of the divalent ion to the sulfonate moiety in NaAMPS and the possibility of intramolecular ion complexation of the divalent ion to the pendent NaAMB side-chain, preventing formation of insoluble ionic bonds.<sup>4</sup>

The subject of this work was to investigate homopolymers of NaAA, NaAMB, and NaAMPS to determine the relative binding characteristics of cations, Na<sup>+</sup>, K<sup>+</sup>, Mg<sup>++</sup>, and Ca<sup>++</sup>, and to elucidate structural influence on macroscopic solution behavior (i.e., viscosity and phase separation). In particular, we wished to ascertain differences in binding characteristics of carboxylate or sulfonate functional groups near to or removed from the polymer backbone. Comparison of the behavior between homopolymers of NaAA, NaAMB, and NaAMPS have thus been made. <sup>23</sup>Na nuclear magnetic resonance (NMR) relaxation rate studies have been performed on these polymers both with and without added electrolytes. <sup>23</sup>Na NMR measurements of poly(sodium galacturonate) (NaGAL) with added Mg<sup>++</sup> and Ca<sup>++</sup> are also included since specific differences in the binding of ions are known to occur. Viscosity profiles of NaAMB and NaAMPS in the presence of each of the salts are presented as well as phase behavior studies on NaAA and NaAMB.

The <sup>23</sup>Na relaxation rates for the polyion systems studied in this work have been employed to yield correlation times,  $\tau_c$ , by employing a theoretical estimate for the fraction of bound monovalent ions,  $P_b$ , in the presence of excess divalent ions. Correlation times were then utilized to obtain values for the quadrupolar coupling constant,  $\chi$ . Values for  $P_b$  for Na<sup>+</sup> in the presence of excess divalent ions were determined using the Manning two-variable theory,<sup>15</sup> which has been demonstrated to be qualitatively descriptive of the fraction of ions bound in the presence of divalent ions.

<sup>23</sup>Na nuclei are well suited for the study of cation binding behavior to electrolytes due to a 100% natural abundance and a high magnetogyric ratio that allow observation by NMR. The sodium ion has a spin 3/2 nucleus in which relaxation is dominated by quadrupolar effects in solution. The relaxation rates,  $R_1$  and  $R_2$ , are sensitive to changes that affect the overall motion

in solution and to electric field gradients (efg) about the nuclei.  $^{23}\text{Na}$  relaxation rate measurements and chemical shift values thus provide a means for investigation of cation binding to polyelectrolytes<sup>17,36-45</sup> and observation of conformational changes that may occur as the degree of ionization along the polymer backbone increases.<sup>41,43,46,47</sup>

The results for  $^{23}\text{Na}$  NMR relaxation studies have generally been interpreted using a two-site model for the observed linewidths or relaxation rates.<sup>17,36,41,43</sup> The two-site model is justified when the exchange rate for the  $\text{Na}^+$  nuclei between the polyanion and bulk solution is faster than the NMR observation time, usually the case for the sodium salts of polyanions. The observed relaxation rates are, therefore, an average of the relaxation rates for the unbound fraction ( $P_F$ ) or free sodium nuclei and the fraction of ions bound ( $P_b$ ) to the polymer,

$$R_{1, \text{obs}} = P_F R_{1, F} + P_b R_{1, b} \quad (1)$$

$$R_{2, \text{obs}} = P_F R_{2, F} + P_b R_{2, b} \quad (2)$$

The magnitude of the relaxation rate depends on the strength of the *efg* experienced by the sodium nuclei at the polyion surface, the lifetime of the  $\text{Na}^+$  at the site, and the number of the sodium nuclei that are bound.<sup>42</sup> The longitudinal and transverse relaxation rates generally display single exponential behavior of the intensity of the NMR signal ( $M_{\text{Obs}}$ ) as a function of  $t$ , the relaxation delay.

$$M_{L, \text{obs}}(t) - M_{L, 0} = (M_L(0) - M_{L, 0}) \exp^{-R_1 t} \quad (3)$$

$$M_{T, \text{obs}}(t) = M_T(0) \exp^{-R_2 t} \quad (4)$$

This is a result of the rapid motion and reorientation of the sodium nuclei such that  $\omega\tau_c < 0.25$  and consequently,  $R_1 = R_2$ . Under conditions of fast exchange and  $\omega\tau_c > 1.5$ <sup>42</sup>,  $R_1$  is no longer equal to  $R_2$ , and the relaxation rates become biexponential decays of the intensity of the NMR transition and the relaxation delay,  $t$ .<sup>48</sup>

$$M_{L, obs}(t) = M_L(0) 0.6 \exp^{-R_2 t} + M_{L, 0}(0) 0.4 \exp^{-R_1 t} \quad (5)$$

Here  $R_{2f}$  and  $R_{2s}$  refer to the fast and slow components of the relaxation decay. In practice, only the transverse relaxation has been observed to display significant biexponential decay with the longitudinal relaxation having single exponential behavior.<sup>44,47</sup> When  $0.25 < \omega\tau_c < 1.5$ , the biexponential behavior is diminished but the relaxation rates are approximately exponential with  $R_1 \neq R_2$ . Under these conditions,  $\tau_c$  can be obtained from the ratio of  $R_1$  to  $R_2$ .<sup>36,47</sup>

### Materials

2-Acrylamido-2-methylpropanesulfonate (AMPS) was washed repeatedly with 2-propanol to remove impurities and vacuum dried at 30 °C before use. All salts (KCl, NaCl, CaCl<sub>2</sub>, MgCl<sub>2</sub>, Mg(NO<sub>3</sub>)<sub>2</sub>, and Ca(NO<sub>3</sub>)<sub>2</sub>) were 99.98% purity or greater and were purchased from Aldrich Chemical Company. Potassium persulfate was obtained from Aldrich Chemical Co. and was recrystallized in water prior to use. 3-Acrylamido-3-methylbutanoic acid (AMB) was synthesized via a Ritter reaction using acrylonitrile and 3,3-dimethylacrylic acid in the presence of water and excess sulfuric acid.<sup>50</sup> Polygalacturonic acid (MW between 25-50,000 g/mole) was purchased from Fluka.

### Polymer Synthesis

Polymers of NaAA, NaAMB, or NaAMPS were prepared at a concentration of 0.45 M by free radical initiation in water at 30 °C using potassium persulfate. After dissolution of the monomer, the pH of the solution was adjusted to 9 by addition of NaOH to insure that the monomer was present in the ionized form (NaAMB and NaAMPS). Excess NaOH was used in the polymerization of NaAA to minimize chain end repulsion to yield a higher MW. The mixture was purged with nitrogen for 20 minutes before initiation with an appropriate amount of potassium persulfate (0.1 mole percent). After 4-6 hours, the reaction mixture was diluted with 2-4 volumes of H<sub>2</sub>O followed by precipitation of the polymer in reagent grade acetone while

stirring. The polymer was washed repeatedly with excess acetone and vacuum dried at 40°C before dissolution into H<sub>2</sub>O. The aqueous polymer solution was dialyzed in water for one week before freeze-drying. The polymer was vacuum dried at 40°C overnight and stored under desiccant. Polymer conversions were approximately 50%. The molecular weights of NaAMB and NaAMPS homopolymers were approximately  $3 \times 10^6$  g/mole.<sup>51</sup> The viscosity average MW of the NaAA homopolymer was estimated from the Mark-Houwink parameters to be approximately  $6 \times 10^5$  g/mole.

Poly(sodium galacturonate) (NaGAL) was prepared by neutralization with NaOH to pH 7.7. Dialysis was performed to remove excess salt.<sup>35</sup> Given the temporal nature of gel formation<sup>34</sup>, Ca<sup>++</sup>/NaGAL solutions were allowed at least 30 minutes to reach equilibrium and were checked at regular intervals over the course of 24 hrs for changes in the <sup>23</sup>Na relaxation rates.

### **NMR, Viscosity, and Phase Separation Measurements**

Sodium NMR measurements were conducted at 25°C with a Bruker MSL-400 operating at 105.6 MHz for <sup>23</sup>Na nuclei.

All polymers were vacuum-dried overnight at 40°C prior to use. Salts were vacuum-dried at 80°C and 5 Torr pressure before use. Polymer solutions were prepared at 0.1 g/dL concentration with 5% D<sub>2</sub>O to provide a frequency lock. The polymer concentration was chosen for these studies to provide a good signal-to-noise with a reasonable number of scans and a reasonably low solution viscosity. Solution volumes for the NMR measurements were 4 mL. Salt solutions were prepared at concentrations between 0.25 and 1M to cover a range of cation/polymer ratios on an equivalent basis. The maximum volume addition to a polymer solution was 200  $\mu$ L. Addition of an equivalent amount of H<sub>2</sub>O to a control polymer solution resulted in no change in the relaxation rate of the Na<sup>+</sup> ions due to dilution effects.  $R_1$  and  $R_2$  measurements on similar concentrations of NaCl solutions were found to have values of 17.3 and 30.3 sec<sup>-1</sup>, respectively, and were employed in all calculations involving  $R_1$  and  $R_2$ . The relaxation rates for the monomers, NaAA, NaAMB, and NaAMPS, were also measured and were

close to those values for sodium chloride. The natural linewidth of a sodium counterion is  $16.7 \text{ sec}^{-1}$  and this value is used in all calculations involving  $R_{2s}$  and  $R_{2f}$ .<sup>47</sup> All calculations and curve fitting were performed with the commercial software program Mathcad®. The experimental errors on the plots are the errors about the mean at the 95% confidence level.

Viscosity measurements were conducted on a Cannon-Fenske capillary viscometer at  $25^\circ\text{C}$  and a polymer concentration of  $0.1 \text{ g/dl}$ . Polymer solutions were aged for at least one month prior to measurement. Phase separation studies were performed on a Brinkmann PC-800 colorimeter using solutions identical to those employed in the viscosity measurements.

## Results and Discussion

Interpretation of the  $^{23}\text{Na}$  NMR measurements require the condition of fast exchange such that the observed relaxation rates are an average of the bound and unbound  $\text{Na}^+$  ions (two-site model). This was verified as an increase in  $R_{2s}$  with reciprocal of temperature (Figure 2), as described by Grasdalen and Kvam<sup>36</sup> and has been reported for a number of polyelectrolytes.<sup>36,37,44,47</sup> The relaxation data are plotted versus the ratio of the number of equivalents of added salt to the number of charged polymer sites.

Biexponential relaxation rates were observed to be time-dependent in solutions of NaAA, NaAMB, and NaAMPS, with  $R_{2f}$  decreasing slightly to a constant value over the course of approximately one month. This behavior is reminiscent of the time-dependency in the viscosity of NaAMB<sup>2</sup> and is consistent with initial clustering of polymer chains upon dissolution that slowly deaggregate. Polymer solutions, stored in polypropylene containers to eliminate the possibility of  $\text{Na}^+$  ions diffusing into the solutions from glass, behaved the same as those stored in glass containers. The increase in biexponential relaxation ( $\Delta R_2 = R_{2f} - R_{2s}$ ) with decreasing polymer concentration for NaAA correlated with that predicted by Halle et al.<sup>37</sup>  $\Delta R_2$  with no added salt is approximately  $140 \text{ Hz}$  for the polymer concentration ( $0.011 \text{ M}$ ) employed in this work.<sup>37</sup>

The behavior of  $R_2$  for sodium counterions with NaAA in the presence of added  $\text{Na}^+$  and  $\text{K}^+$  is shown in Figure 3. The effect of added  $\text{Na}^+$  on  $R_1$  is also shown. The  $R_1$  data for  $\text{K}^+$  and the single exponential fits to the transverse relaxation are not presented to avoid further confusion

on the plots. The  $R_1$  data for  $K^+$  are nearly identical to those for  $Na^+$ . The experiments by Leyte and coworkers demonstrated that the biexponential behavior of sodium(polystyrenesulfonate), NaPSS, diminished as the concentration of added NaCl increased to approximately twice the polymer concentration.<sup>37,44</sup> In Figure 3,  $R_{2f}$  and  $R_{2s}$  reach similar values at  $C_{salt}/C_p \approx 3$ . Biexponential relaxation of NaAA with added  $Na^+$  and  $K^+$  is nearly identical, indicating similar binding of the ions to NaAA.

## References

1. McCormick, C.L. *J. Macromol. Sci. Polym. Chem. Ed.* **1985**, A-22, 955.
2. McCormick, C.L.; Blackmon, K.P.; Elliot, D.L. *J. Polym. Sci. Part A: Polymer Chem.* **1986**, 24, 2619.
3. McCormick, C.L.; Elliot, D.L. *Macromol.* **1986**, 19, 542.
4. McCormick, C.L.; Elliot, D.L. *J. Polym. Sci. Polym. Chem. Ed.* **1987**, 25, 1329.
5. McCormick, C.L.; Middleton, J.C.; Cummings, D.C. *Macromol.* **1992**, 25, 1201.
6. Ikegami, A.; Imai, N. *J. Polym. Sci.* **1962**, 56, 133.
7. Travers, C.; Marinsky, J.A. *J. Polym. Sci. Symp.* **1974**, 47, 285.
8. Michaeli, I. *J. Polym. Sci.* **1960**, 48, 291.
9. Schwartz, T.; Francois, J. *Makro. Chem.* **1981**, 182, 2775.
10. Truong, D.N.; Galin, J.C.; Francois, Q.T. *Polym. Comm.* **1984**, 25, 208.
11. Arai, F. Master's Thesis, University of Southern Mississippi, Hattiesburg, MS, 1984.
12. Carroll, W.R.; Eisenberg, H. *J. Poly. Sci.: Part A-2* **1966**, 4, 599.
13. Hen, J.; Strauss, U.P. *J. Phys. Chem.* **1978**, 78, 1013.
14. Eisenberg, H.; Mohan, G.R. *J. Phys. Chem.* **1959**, 63, 71.
15. Manning, G.S. *Quart. Rev. Biophys. II* **1978**, 2, 179.
16. Morawetz, H., "Macromolecules in Solution", **1983**, Robert E. Krieger Publishing Co., Malabar, FL.
17. Qian, C.; Asdojodi, M.R.; Spencer, H.G; Savitsky, G.B. *Macromol.* **1989**, 22, 995.
18. (a) Fuoss, R.M.; Katchalsky, A.; Lifson, S. *Proc. Nat. Acad. Sci.* **1951**, 37, 579. (b) Alfrey, T.; Berg, P.W.; Morawetz, H. *J. Poly. Sci.* **1951**, 7(5), 543. (c) Katchalsky, A. *Pure Appl. Chem.* **1971**, 26, 327.
19. Joshi, Y.M.; Kwak, J.C.T. *Biophys. Chem.* **1981**, 13, 65.
20. Mattai, J.; Kwak, J.C.T. *Biochim. et Biophys. Acta* **1986**, 677, 303.
21. Mattai, J.; Kwak, J.C.T. *Macromol.* **1986**, 19, 1663.
22. Strauss, U.P.; Leung, Y.P. *J. Amer. Chem. Soc.* **1965**, 87(7), 1476.
23. Begala, J.A.; Strauss, U.P. *J. Phys. Chem.* **1972**, 76(2), 254.
24. Ikegami, A. *J. Poly. Sci.: Part A* **1964**, 2, 907.
25. Satoh, M.; Hayashi, M.; Komiyama, J.; Iijima, T. *Polymer* **1990**, 31, 501.
26. Satoh, M.; Kawashima, T.; Komiyama, J. *Polymer* **1991**, 32, 892.
27. Satoh, M.; Hayashi, M.T.; Komiyama, J.; Iijima, T. *Polym. Comm.* **1988**, 29, 49.
28. Tan, J.S; Marcus, P.R. *J. Poly. Sci.: Poly. Physics Ed.* **1976**, 14, 239.

29. Lips, A.; Clark, A.H.; Cutler, N.; Durand, D. *Food Hydrocolloids* **1991**, *5*, 87.
30. Rinaudo, M; Milas, M. *J. Poly. Sci.: Poly. Chemistry Ed.* **1974**, *12*, 2073.
31. Grant, G.T.; Morris, E.R.; Rees, D.A.; Smith, P.J.C.; Thom, D. *FEBS Letters* **1973**, *32(1)*, 195.
32. Morris, E.R.; Rees, D.A.; Thom, D.; Boyd, J. *Carbo. Res.* **1978**, *66*, 145.
33. Morris, E.R.; Powell, D.A.; Gidley, M.J.; Rees, D.A. *J. Mol. Biol.* **1982**, *155*, 507.
34. Powell, D.A.; Morris, E.R.; Gidley, M.J.; Rees, D.A. *J. Mol. Biol.* **1982**, *155*, 517.
35. Thibault, J.F.; Rinaudo, M. *Biopolymers* **1986**, *25*, 455.
36. Grasdalen, H.; Kvam, B.J. *Macromol.* **1986**, *19*, 1913.
37. Halle, B.; Wennerstrom, H.; Picullel, L. *J. Phys. Chem.* **1984**, *88*, 2482.
38. Moss, F.M.; Spencer, H.G.; Savitsky, G.B.; Reidl, C.M. *Polymer* **1991**, *32*, 1504.
39. Nagarkar, G.S.; Kotun, M.; Savitsky, G.B.; Spencer, H.G. *Polym. Comm.* **1991**, *32*, 486.
40. Riedl, C.; Qian, C.; Savitsky, G.B.; Spencer, H.G; Moss, W.F. *Macromol.* **1989**, *22*, 995.
41. Gustavvson, H.; Siegel, G.; Lindman, B.; Fransson, L. *Biochimica et Biophysica Acta* **1981**, *677*, 23.
42. Forsen, S.; Lindman, B. *Chem. Brit.* **1978**, *14*, 29.
43. Siegel, G.; Walter, A.; Bostanjoglo, M.; Jans, A.W.H.; Kinne, R.; Picullel, L.; Lindman, B. *J. Membr. Sci.* **1989**, *41*, 353.
44. Levij, M.; De Bleijser, J.; Leyte, J. *Chem. Phys. Lett.* **1981**, *83(1)*, 183.
45. Gunnarsson, G.; Gustavvson, H. *J. Chem. Soc. Faraday. Trans. I* **1982**, *78*, 2901.
46. Gustavvson, H.; Lindman, B.; Tornell, B. *Chemica Scripta* **1978**, *10*, 136.
47. Gustavvson, H.; Lindman, B. *J. Amer. Chem. Soc.* **1978**, *100(15)*, 4647.
48. Bull, T.E. *J. Mag. Res.* **1972**, *8*, 344.

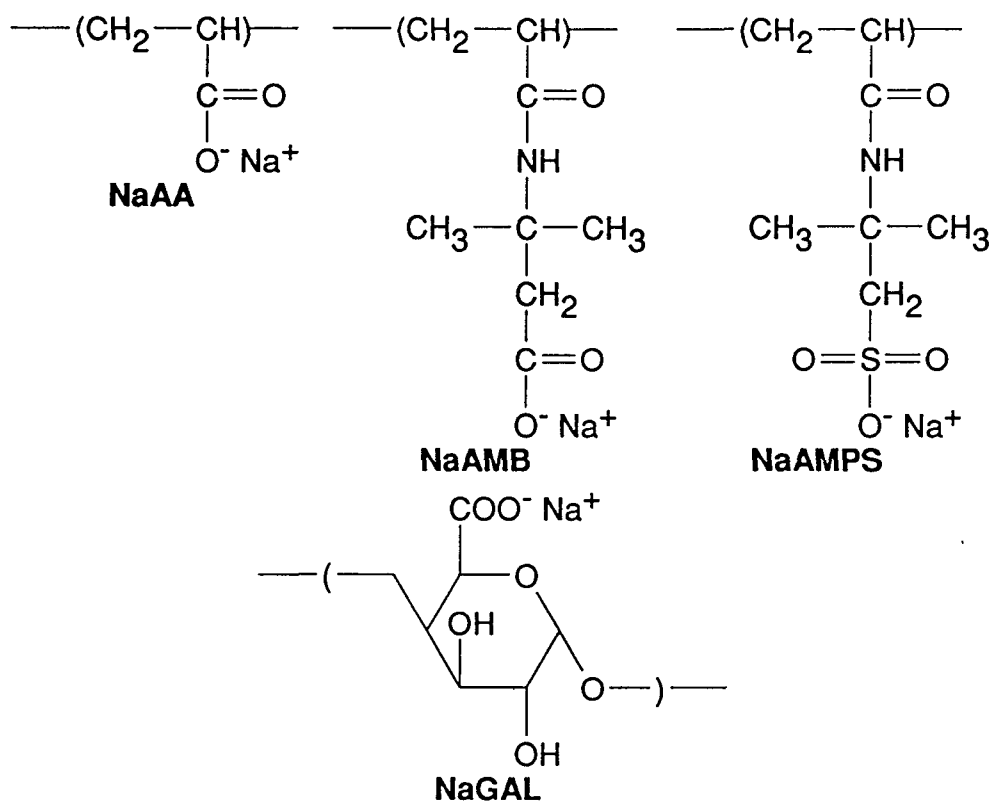


**Figure 1.** Structure of copolymers employed in NMR study.

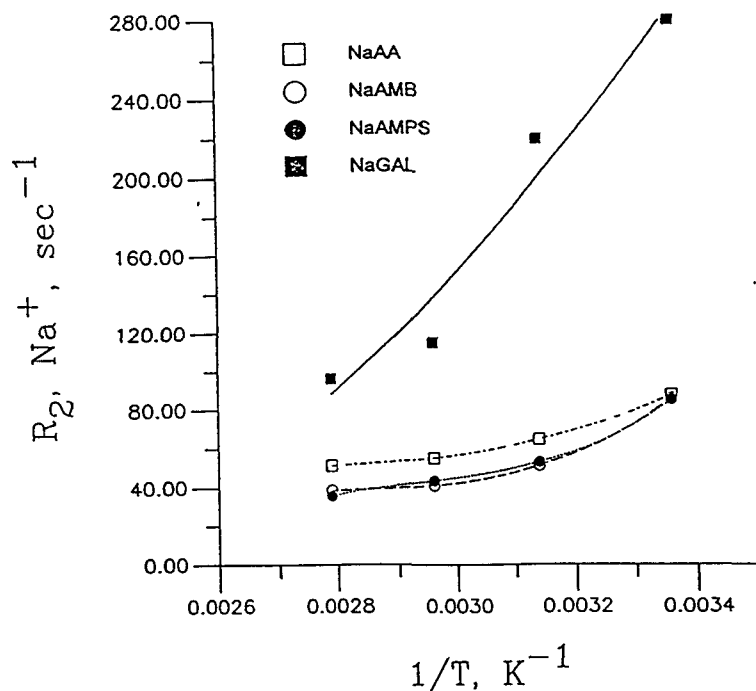


**Figure 2.** Slow component of the relaxation rate,  $R_{2s}$ , of NaAA, NaGAL, NaAMB, and NaAMPS as a function of temperature at a polymer concentration of 0.1 g/dl.

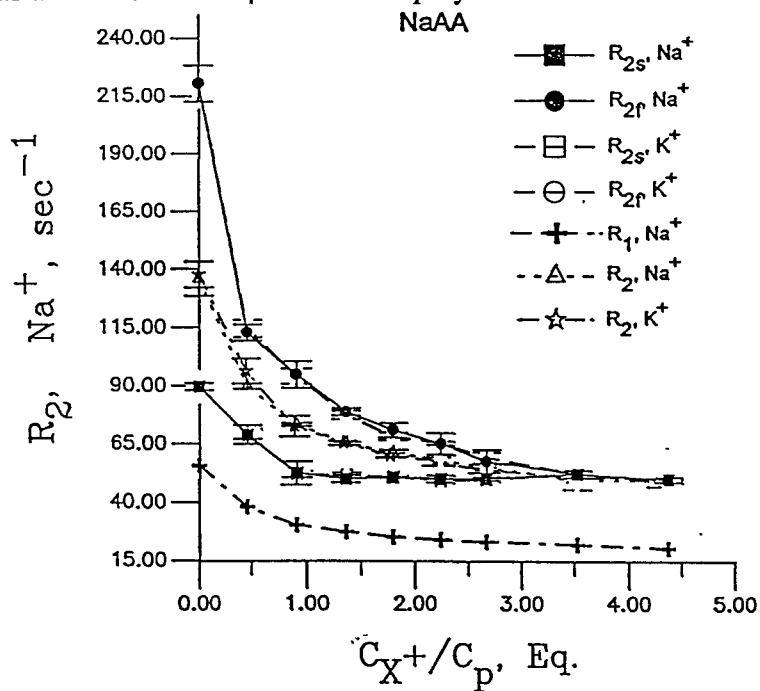


**Figure 3.** Longitudinal ( $R_1$ ) and transverse ( $R_{2s}$  and  $R_{2f}$ ) relaxation rates of NaAA with increasing  $\text{Na}^+$  and  $\text{K}^+$  concentration. The polymer concentration is 0.1 g/dl.

## B. Task 2. $^{23}\text{Na}$ NMR Studies of Hydrophobically Modified Polyacids

Hydrophobic modification of polyelectrolytes can impart desirable properties to copolymers in aqueous solution. For example, hydrophobic substituents of properly-tailored systems can associate in aqueous solution to form microheterogeneous domains. "Closed" or intramolecular associations may induce surface active qualities while "open" or intermolecular associations may lead to viscosification in aqueous media. The organization of the microheterogeneous associates and responsiveness to changes in pH and ionic strength dictate the usefulness of such systems in applications ranging from phase transfer to rheology modification. An external probe such as naphthalene or pyrene can be solubilized within these microheterogeneous zones and dynamic information about the environment may be obtained from fluorescence studies. Incorporation of the chromophore as a hydrophobic label allows examination of the internal dynamics of hydrophobically-modified polyelectrolyte systems.<sup>1-5</sup>

Poly(methacrylic acid) (PMA) exhibits conformational reordering as the degree of ionization,  $\alpha$ , along the polymer backbone reaches a critical value.<sup>6</sup> The methyl groups associate at low pH, forming a compact coil (hypercoil) with hydrophobic domains. As the degree of ionization increases, coulombic repulsions overcome weak associations of the methyl groups, expanding the coil. This conformational transition has been observed by fluorescence techniques<sup>6,7</sup> as well as classical methods<sup>8</sup>. Hydrophobically-modified poly(methacrylic acid) has been reported to adopt a "hypercoiled" structure in which the hydrophobes form an inner hydrophobic domain surrounded by ionized carboxylate units.<sup>9,10</sup> These hypercoils may persist even at high degrees of ionization if the pendent hydrophobes have flexible spacers.<sup>1,2,10,11</sup>

The major objective of this work was to investigate via  $^{23}\text{Na}$  NMR the behavior of sodium hydroxide-neutralized acrylic and methacrylic acid copolymers which have been prepared with one and ten mole % 2-(1-naphthylacetamido)ethylacrylamide (NAEAM) comonomer (Figure 1). The NAEAM comonomer serves a dual purpose of acting as a "hydrophobe" and a fluorescence label. A further objective of this work was to ascertain whether or not the  $^{23}\text{Na}$

NMR method might be useful in probing the pH-responsive domain organization deduced from previous photophysical and viscometric studies.<sup>1,2</sup>

## Experimental

Sodium NMR measurements were conducted at 25°C on a Bruker MSL-400 operating at 105.8 MHz for  $^{23}\text{Na}$  nuclei. Longitudinal relaxation rates ( $R_1$ ) were measured using the inversion-recovery method. All curves were observed to be single exponential decays and were fit to Equation 5 (see Introduction of previous paper) using the Bruker SIMFIT program. Transverse relaxation rates ( $R_2$ ) were measured (non-spinning) using the Carr-Purcell-Meiboom-Gill (CPMG) pulse sequence and were fit to Equations 5 and 6. Since no previous criteria have been established for the determination of the onset of biexponential relaxation behavior, we have arbitrarily chosen a cutoff for the onset of biexponentiality as being the point where the error of the fit of Equation 5 exceeded that of Equation 6 by 10%. Error bars on the plots are given at the 95% confidence level.

The synthesis of the copolymers (Figure 1) has been previously<sup>2</sup> described with the mole percent of NAEAM incorporated as follows: 0.9% NAEAM in PAA (NAA-1), 9.3% NAEAM in PAA (NAA-10), 1.02% NAEAM in PMA (NMA-1), and 11.8% NAEAM in PMA (NMA-10). Poly(acrylic acid) (PAA, MW=250,000 g/mole) and poly(methacrylic acid) (PMA, MW=15,000 g/mole) were obtained from Polysciences, Inc. Polymer solutions were prepared to 0.1 g/dL concentration with 5% D<sub>2</sub>O to provide a frequency lock. The polymer concentration for these studies was selected to provide a good signal-to-noise ratio with a reasonable number of scans and to fall within the dilute regime in order to minimize possible associative interactions between isolated polymers. The polymers were initially prepared at pH 9 and titrated with 1M HCl to the desired pH values. Attempts to titrate from an acidic polymer solution using NaOH were unsuccessful due to the insolubility of the 10% NAEAM-labelled polymers at low pH. The degree of ionization was determined from the amount of added acid.

## Results and Discussion

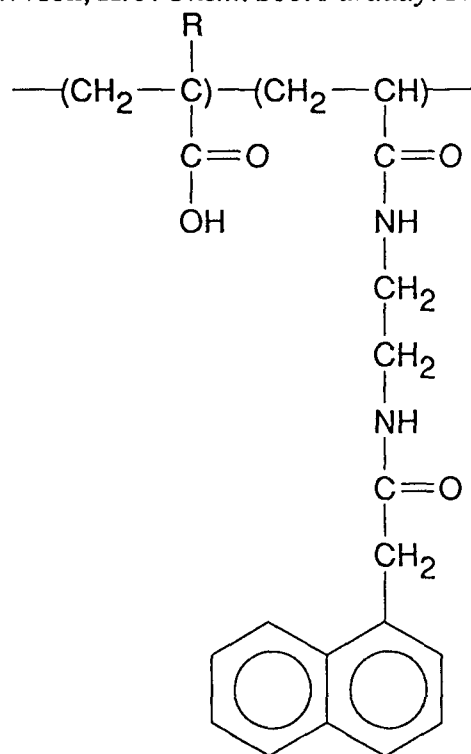
In the following discussion, the longitudinal and transverse relaxation rates of PAA, PMA, and the labelled, hydrophobically-modified NAA and NMA series (Figure 1) will be presented.<sup>2</sup> The slow and fast transverse relaxation rates,  $R_{2s}$  and  $R_{2f}$ , respectively, are included when the relaxation decays displayed biexponential character at low  $\alpha$ . At  $\alpha$  values above 0.8, biexponential rate behavior was observed; however, these data are not presented since the region of interest for this study are  $\alpha$  values less than approximately 0.8. Correlation times,  $\tau_c$ , are calculated from  $\Delta(R_1/R_2)$  since  $\omega\tau_c > 0.25$  over the range of all  $\alpha$  values. For the NMA series, the biexponential relaxation rates observed at low  $\alpha$  were also employed to calculate  $P_b\chi^2$ .

In Figure 2, the transverse and longitudinal relaxation rates for NAA-1 are plotted as a function of the degree of ionization.  $R_1$  and  $R_2$  values are nearly identical for NAA-1 and PAA. Also the values for the latter are consistent with those from previous studies.<sup>13</sup> In Reference 13,  $R_2$  has slightly higher values than  $R_1$  indicating that  $\omega\tau_c > 0.25$ .<sup>11</sup> The data presented in our work also demonstrate that  $\omega\tau_c > 0.25$  as evidenced by the inequality of  $R_1$  and  $R_2$  over the range of pH values studied. Both relaxation rates increase smoothly towards  $\alpha = 1$ . The similarity in the relaxation rates for PAA and NAA-1 demonstrates that incorporation of 1% NAEAM has no observable effect on the  $^{23}\text{Na}$  NMR behavior.

Figure 3 illustrates the dependence of  $R_1$  and  $R_2$  on  $\alpha$  for NAA-10. The behavior is quite different from that observed in PAA and NAA-1. Below  $\alpha = 0.5$ ,  $R_2$  can be resolved into slow and fast ( $R_{2s}$  and  $R_{2f}$ ) components. It is interesting to note that a substantial decrease in  $R_2$  and  $R_{2f}$  is matched by a marked increase in  $I_E/I_M$  (the fluorescence intensity ratio of excimer to monomer designated by the stars in Figure 3) as  $\alpha$  approaches 0.5. These superimposed data are from previous studies<sup>2</sup> on this polymer by our group. This behavior is consistent with the adoption of a pseudomicellar conformation with high values of  $I_E/I_M$ .<sup>2</sup> The "micellelike" or hypercoil structure persists at still higher values of  $\alpha$  up to 0.7, beyond which  $R_2$  increases dramatically and  $I_E/I_M$  decreases slightly. The number of ions bound and the strength of the binding in the "hypercoil" play roles in the observed changes.

## References

1. McCormick, C.L., Hoyle, C.E., and Clark, M.D. *Macromolecules*, **1990**, 23, 3124.
2. McCormick, C.L., Hoyle, C.E., and Clark, M.D. *Macromolecules*, **1991**, 24, 2397.
3. Guillet, J.E., Wang, J., and Gu, L. *Macromolecules*, **1986**, 19, 2793.
4. Bai, F., Chang, C.-H., and Webber, S.E., *Photophysics of Polymers*; Hoyle, C.E. and Torkelson, J.M., Eds., ACS Symposium Series 385, American Chemical Society, Washington, D.C., **1987**.
5. Chu, D.-Y and Thomas, J.K., *Macromolecules*, **1984**, 17, 2142.
6. Chen, T.S. and Thomas, J.K., *J. Polym. Sci. Polymer Chemistry Edition*, **1979** 17, 1103.
7. Olea, A.F. and Thomas, J.K., *Macromolecules*, **1989**, 22, 1165.
8. Kotliar, A.M. and Morawetz, H., *J. Am. Chem. Soc.*, **1955**, 77, 3692; Crescenzi, V., Quadrifoglio, F., and Delben, F., *J. Polym. Sci.*, **1972**, A-2, 10, 357.
9. Guillet, J.E. and Rendall, W.E., *Macromolecules*, **1986**, 19, 224.
10. Holden, D.A., Rendall, W.E., and Guillet, *Ann. N.Y. Acad. Sci.*, **1981**, 366, 11.
11. Gustavvson, H., and Lindman, B., *J. Amer. Chem. Soc.*, **1978**, 100(15), 4647.
12. Song, D.J. and Jhon, M.S., *Polymer*, **1993**, 100, 1687.
13. Gunnarsson, G. and Gustavvson, H. *J. Chem. Soc. Faraday. Trans. I*, **1982**, 78, 2901.



**R = -H: NAA-1, 10**

**R = -CH<sub>3</sub>: NMA-1, 10**

**Figure 1.** Structures of the NAA and NMA copolymers.

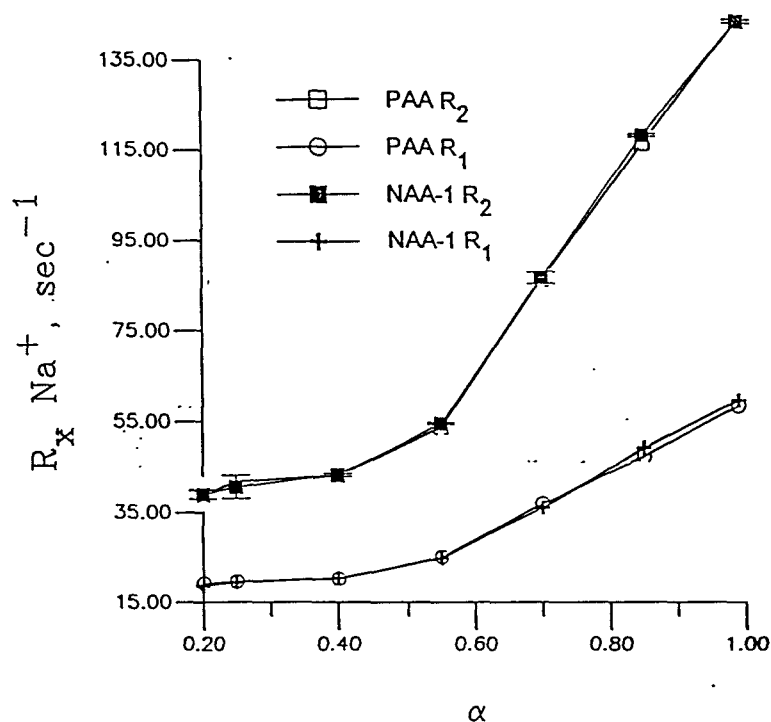


Figure 1. Transverse ( $R_2$ ) and longitudinal ( $R_1$ ) relaxation rates of PAA and NAA-1 with increasing  $\alpha$ . The polymer concentration is 0.1 g/dl.

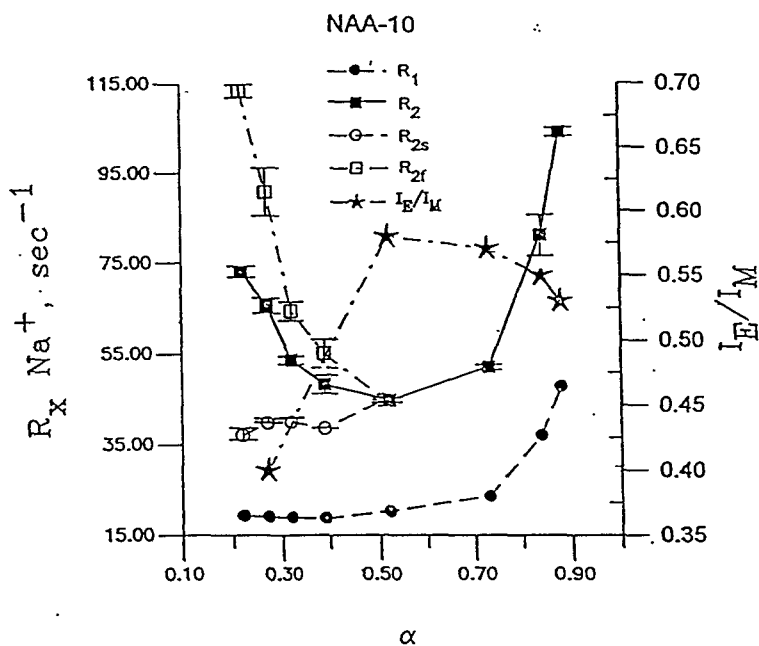


Figure 3. Transverse ( $R_2$ ) and longitudinal ( $R_1$ ) relaxation rates of NAA-10 with increasing  $\alpha$  along with the biexponential transverse relaxation rates ( $R_{2s}$  and  $R_{2f}$ ). The ratio of excimer to monomer fluorescence emission,  $I_E/I_M$ , is also depicted. The polymer concentration is 0.1 g/dl.

### C. Task 3 - Solution Rheology

#### NaAMB / AM Copolymer Solution Flow Behavior in Porous Media

##### Introduction

When using a dilute polymer solution to flood an oil reservoir the displacing fluid should have a high resistance to flow within the porous medium. High flow resistance increases movement of residual oil to a producing well and thus enhances oil recovery. Fluid resistance results from polymer coil molecular distortions during flow through the small and tortuous channels of the porous medium. Polymer solution behavior in complex porous media can be modeled using packed beds of uniform solid spheres.

As polymer coils in solution pass through a bed of packed spheres of diameter,  $d$ , they travel through a continuous and interconnected series of converging and diverging cavities. The fluid in this geometry will continually accelerate and decelerate as it passes from cavity to cavity. Fluid acceleration and deceleration forces will compel the polymer coils to extend and then contract or recover after each extension. The number of coil extensions and recovery cycles is equal to the number of cavities passed through by the polymer in a given time.

Each coil extension-recovery cycle will convert some fluid kinetic energy into heat. This energy conversion will be sensed as a higher solution pressure drop across the bed,  $\Delta P$ , as compared to the pressure drop of a solvent flowing through the bed at the same flow conditions. This fluid pressure increase is expressed as a Normalized Flow Resistance,  $\psi$ .

The Normalized Flow Resistance,  $\psi$ , is directly related to the amount of energy converted to heat by the polymer coils as they travel through the packed bed and are continually extended and contracted. Thus Durst Plots, which show the Normalized Flow Resistance versus Deborah Number, show the efficiency that polymer coils convert kinetic energy to heat as a function of flow conditions, porous media geometry, and polymer properties and concentration.

The Normalized Flow Resistance,  $\psi$ , measures solution flow resistance in a porous media under conditions specified by the Reynolds and Deborah Numbers. It is calculated from the friction factor of the solution,  $f$ , and the friction factor of the solvent,  $f_s$ , measured at the same bed Reynolds number. The Deborah Number,  $De$ , is the product of the polymer coil response time,  $\tau$ , and the average fluid extension rate,  $\epsilon$ , which depend upon average fluid velocity and the pore geometry. These dimensionless parameters are defined by the relationships given below.

$$D_e = \epsilon \lambda \quad \psi = \frac{f - f_s}{f_s [\eta] C}$$

$$e = \frac{\sqrt{2} v}{d \phi} \quad Re \equiv \frac{v d \rho}{\eta_s (1 - \phi)}$$

$$\tau = \frac{\eta_s [\eta] M}{R T} \quad f \equiv \frac{d \phi^3}{v^2 (1 - \phi) \rho} \frac{\Delta P}{\Delta \ell}$$

As shown in the above equations, the nature of the porous medium is specified by the diameter of the spherical particles,  $d$ , forming a bed having porosity,  $\phi$ . The fluid flow resistance through the bed is measured by the pressure drop per unit length of bed,  $\Delta P / \Delta \ell$ . Flow conditions through the bed are defined by the average fluid velocity,  $v$ . This velocity is based on the cross sectional area of an empty bed. The fluid velocity within the pore channels within the bed would be the empty bed velocity divided by the bed porosity. Solution properties of shear viscosity,  $\eta_s$ , and density,  $\rho$ , are also used in the dimensionless groups. The coil response time,  $\tau$ , can be estimated from the intrinsic viscosity of the polymer,  $[\eta]$ , its molecular weight,  $M$ , and the temperature,  $T$ .

Past experimental work has shown that as the Deborah Number approaches unity a maximum solution flow resistance develops and is maintained at higher Deborah Numbers<sup>4</sup>. The maximum in the Normalized Flow Resistance is expected to be a function of polymer molecular weight, macromolecular structure and the concentration of polymer coils in solution.

## **Experimental**

### Polymers

The high molecular weight random copolymers used in this study were synthesized from acrylamide (AM) and 3-acrylamido-3-methylbutanoic acid (AMBA) monomers in the ratio as described in previous publications<sup>1,2</sup>. Four copolymers in the solid form were synthesized having AM/ NaAMB monomer ratios of 5/95, 10/90 ( two samples of different molecular weights ), and 20/80. The aqueous solvent used to make all polymer solutions contained 0.514 M NaCl and had a viscosity of 0.934 cp at 25 ° C.

Solutions of these copolymers were analyzed using static and dynamic light scattering characterization techniques to find coil sizes, molecular weights and Viral coefficients. A low shear Contravis rheometer was used to estimate each solution intrinsic viscosity in the limit of zero shear rates. Table I list polymer properties and the calculated dilute solution coil response times for each polymer.

## Porous Media Rheometer

The porous media rheometer<sup>3</sup> used for this study is shown in Figure 1. Pressurized nitrogen gas forced polymer solution or solvent out of a 1000 ml sample reservoir through one of two porous media flow cells. The fluid flow rate was controlled by adjusting the nitrogen gas pressure with a Victor 0 to 200 psi, single stage, pressure regulator. Both flow cells were 1 cm diameter cylinders having a 12 cm length. The cells were packed with uniform diameter solid glass spheres manufactured by Cataphote Inc. Cell # 1 contained 297 micron diameter glass spheres. Cell # 2 contained 149 micron diameter glass spheres. Both packed beds had a porosity,  $\phi$ , of 0.367. Fluid from a flow cell was directed into a flask that was placed upon a Mettler PM4000 balance. The fluid mass throughput was measured by recording the change in mass on the balance with respect to time.

The glass spheres were retained within the flow cells at each end by three polypropylene screens having mesh sizes of 149, 390, and 149. A threaded retaining plug, having 25 through holes, each having a diameter of 0.07 cm, was used at each flow cell end to compress the screens against the glass spheres. Each cell end was capped with a Swagelock SS-400-1-6ST fittings.

Pressure probes were positioned 10 cm apart in both packed beds. Each probe was a 0.159 cm diameter stainless steel tube that had two 0.09 mm wide by 4.2 mm long slit openings. The probes were positioned within the cells such that the slit centered the packed bed. The fluid pressure difference across the probes in each cell was measured using a Validyne DP15 differential pressure transducer with a number 48 diaphragm. The pressure transducers were previously calibrated by applying a hydraulic force across the transducers using a series of known weights. The electrical signals from a pressure transducer (bed fluid pressure drop) and the balance (mass of fluid) were recorded each second by a Camile, model 2000, process controller. The controller graphically displayed both signals as a function of time.

After fluid is forced through the rheometer system by fixing a nitrogen gas pressure, steady state conditions were detected when the Camile real-time plots of flow rate and pressure drop versus time were constant. This usually required about one minute. After the system reached steady state, the pressure drop across the packed bed and the flow rate was averaged for 30 seconds. These averages were then recorded. Thereafter a new nitrogen gas pressure was then set to force fluid through the rheometer at a different mass throughput and the above procedure repeated.

Usually about 12 solvent throughput conditions were used to characterize the porous media flow properties of the solvent. Thereafter polymer solution was forced through the rheometer system over the same range of bed Reynolds numbers. Laminar fluid flow conditions were maintained in all test by always having a bed Reynolds numbers less than 10.

After the polymer solution flow properties were measured, solvent was again forced through the rheometer. This was done to determine if any polymer has been retained in a packed bed. If the porous media flow properties of the second solvent were significantly greater than the first solvent then additional solvent was forced through the rheometer until the second solvent offered the same porous media flow resistance as the first solvent. This purging of a flow cell with solvent

assured that the packed bed was free of polymer and thus could not affect the rheometer measurements on subsequent polymer solutions. After three sets of data were collected (solvent before polymer solution, polymer solution, and solvent after polymer solution), they are imported into a Mathcad 5.0 document where data analysis calculations were performed.

## **Results**

### Durst Plots

As shown by the Durst plots of Figures 2 and 3, all polymer solutions show the same generally expected  $\psi$  versus  $D_e$  relationship when using either cells # 1 or # 2. Recall that cell # 1 and cell # 2 have uniform packed spheres with diameters of 297 and 149 microns, respectively. In these packed beds a converging-diverging channel geometry exists over a distance scale that corresponds to the diameter of a sphere. This geometry forces the fluid velocity to accelerate and decelerate as it passes through the porous media and this produces cyclic extensional and compressional strains on the polymer coils.

As shown by both Figures, at Deborah numbers less than 0.1,  $\psi$  values are usually less than 4. As the Deborah number increases above 0.1, the  $\psi$  values increase to a maximum at a Deborah number of about 0.5. However, in contrast to previous observations<sup>4</sup> the  $\psi$  parameter decreases as the Deborah Number increases to values greater than 0.5. This reduction in the Normalized Flow Resistance at higher Deborah numbers is probably due to the diminished ability of polymer coils to convert kinetic energy to heat as they are extended and compressed at faster rates. At faster fluid flow conditions the polymer coils are not able to follow in concert with the rapidly changing local fluid flow fields because insufficient time is available for coil deformation during fluid acceleration and coil recovery during fluid deceleration. As a consequence, less total coil extension and compression is experienced each cycle and thus less energy is converted into heat by the macromolecules. Therefore the solution will have less resistance to flow through the porous medium at higher Deborah numbers.

### Effects of Polymer Molecular Weight

When the polymer has a low molecular weight, very large fluid velocities are needed in a porous medium to achieve a Deborah Number greater than 0.1. This can be shown by using Figures 2a and 2b to compare the flow performance of low and high molecular weight NaAMB/AM copolymers. For these two copolymers to have the same Deborah Number flow conditions the fluid velocity of the low molecular weight copolymer has to be about 20 times larger than the high molecular weight copolymer. This is because for equal Deborah numbers the fluid velocities must scale to the ratio of the inverse of each copolymer response time (7.8 msec / 0.4 msec = 20).

These results show that low molecular weight polymers would not have significant extensional flow resistance in reservoirs because the fluid velocities at typical flooding conditions away from the injection well are too low to cause coil extension. In contrast, a high molecular weight copolymer coil can be extended in the porous media at much lower fluid velocity and therefore are better candidates for reservoir flooding.

The Normalized Flow Resistance,  $\psi$ , is directly proportional to the difference between solution and solvent friction factors,  $f - f_s$ , and is also inversely proportional to the product of the dimensionless concentration of polymer coils in solution, and solvent friction factor. The dimensionless concentration of polymer coils is the product of the polymer's mass concentration and its intrinsic viscosity,  $C[\eta]$ . Thus  $\psi$  is a measure of the increase in solution flow resistance as compared to solvent per dimensionless concentration of polymer coils in solution. Because higher molecular weight polymers have larger intrinsic viscosities than lower molecular weight polymers (coils occupy more volume per unit mass polymer) then less high molecular weight polymer mass is needed to have the same dimensionless concentration. Thus less mass of a high molecular weight polymer is needed to achieve the same Normalized Flow Resistance,  $\psi$ , when compared to lower molecular weight polymer.

### Effects of Copolymer Monomer Composition

Polymer molecular structure is also important factor influencing solution flow resistance. Figure 3a through 3b show Durst plots of three different NaAMB / AM copolymers. The molecular weights of all three copolymers are about the same, however the difference in copolymer monomer composition has greatly affected the expansion of the polymer coils. The NaAMB / AM 20 / 80 copolymer having 20% NaAMB monomer has an intrinsic viscosity of 46 dl / g. This intrinsic viscosity is 2.5 times greater than the other two copolymers. Also as shown by Table I, the 20 / 80 copolymer has macromolecular coils that are much larger in diameter than the other two copolymers. The 20 / 80 monomer composition has greatly expanded the polymer coils in solution.

When compared to the 3.3 million molecular weight AM homopolymer of Figure 2c, the 14 million molecular weight 20 / 80 copolymer of Figure 3c has a coil response time which is 26 times greater ( 26 msec versus 1 msec ). Thus even at very low porous media fluid velocities the 20 / 80 polymer coils will experience elongation and therefore have a large resistance to flow.

### General Flow Behavior of All Polymer Solutions

All the Durst plots show the same general behavior regardless of polymer type. At Deborah numbers less than about 0.1, the Normalized Flow Resistance is very low which indicates that almost no polymer coil extension and recovery is occurring under these conditions. At Deborah numbers between 0.1 and 0.8, the Normalized Flow Resistance increases to a maximum but then decreases as the Deborah number increases to higher values. This suggests that the degree of polymer coil expansion and recovery is at first accelerating under these conditions, then reaches a limit at a Deborah number of about 0.6. Above this Deborah number the polymer coils are probably not able to completely recover all of the large extensional strains developed during previous extension-recovery cycles. Thus they have less potential to extend in subsequent extension-recovery cycles. Therefore, at higher Deborah numbers the coils travel through the bed in a more extended state. They will have less and less recoverable extension as they travel from cavity to cavity. At very high Deborah Numbers the polymers travel through the bed in a highly extended state and less fluid kinetic energy is converted to heat. Thus, the Normalized Flow Resistance should decrease to zero in the limit of high Deborah numbers.

## Conclusions

Of all the polymer examined, the NaAMB / AM 20 / 80 copolymer solutions had the greatest porous media flow resistance. This is because the polymer coils of these macromolecular structures are greatly expanded and can elongate and recover in extensional flow fields having low average fluid velocities.

The use of high molecular weight, highly expanded copolymers (such as the NaAMB / AM 20 / 80 shown in Figure 3c) versus lower molecular weight polymers that are not greatly expanded (such as the AM homopolymer shown in Figure 2c) has a dual advantage in reservoir flooding. Solutions of larger molecular weight macromolecules with expanded polymer coils not only require less polymer mass for a given fluid flow resistance but this resistance is experienced at lower flow rates through the porous media. Thus they are effective flooding agents even at low concentrations and have a significant economic advantage.

## References

1. McCormick, C. L. , K. P. Blackmon, *J. Poly. Sci., Poly. Chem.*, A24, 2635, 1986.
2. McCormick, C. L., K. P. Blackmon, D. L. Elliott, *J. Poly. Sci., Poly. Chem*, A24, 2619, 1986.
3. McCormick, C. L. and R. D. Hester, "Responsive Copolymers for Enhanced Petroleum Recovery," DE-AC22-92BC-14882, Quarterly Technical Progress Report, June 22, 1993.
4. Durst, F. and R. Haas, *Rheol. Acta*.1981, 20, 179.

**Table I**  
NaAMB / AM Copolymer Solution Properties at 25 °C Using 0.514 M NaCl Aqueous Solvent

Copolymer Monomer Molar Ratio	Intrinsic Viscosity	Diffusional Coeff.	Hydrodynamic Radius	Radius of Gyration	Weight Average Mol. Weight	Second Viral Coeff.	Polymer Coil Response Time
NaAMB : AM	$[\eta]$	$D_{luc} \times 10^8$	$R_h$	$R_g$	$M \times 10^6$	$A_2 \times 10^4$	$\tau$
dimensionless	dl / g	cm <sup>2</sup> / sec	Å	Å	g / mole	ml mole / g <sup>2</sup>	sec x 10 <sup>3</sup>
0 : 100	7.2	–	–	–	3.3	–	1
5 : 95	17	1.3	1800	2950	12	2.8	8.3
10 : 90	4.8	–	–	–	1.9	–	0.4
10 : 90	18	5	460	–	11	–	7.8
20 : 80	46	0.68	3400	3700	14	3.1	26.2

Figure 1: Porous Media Elongational Flow Rheometer System

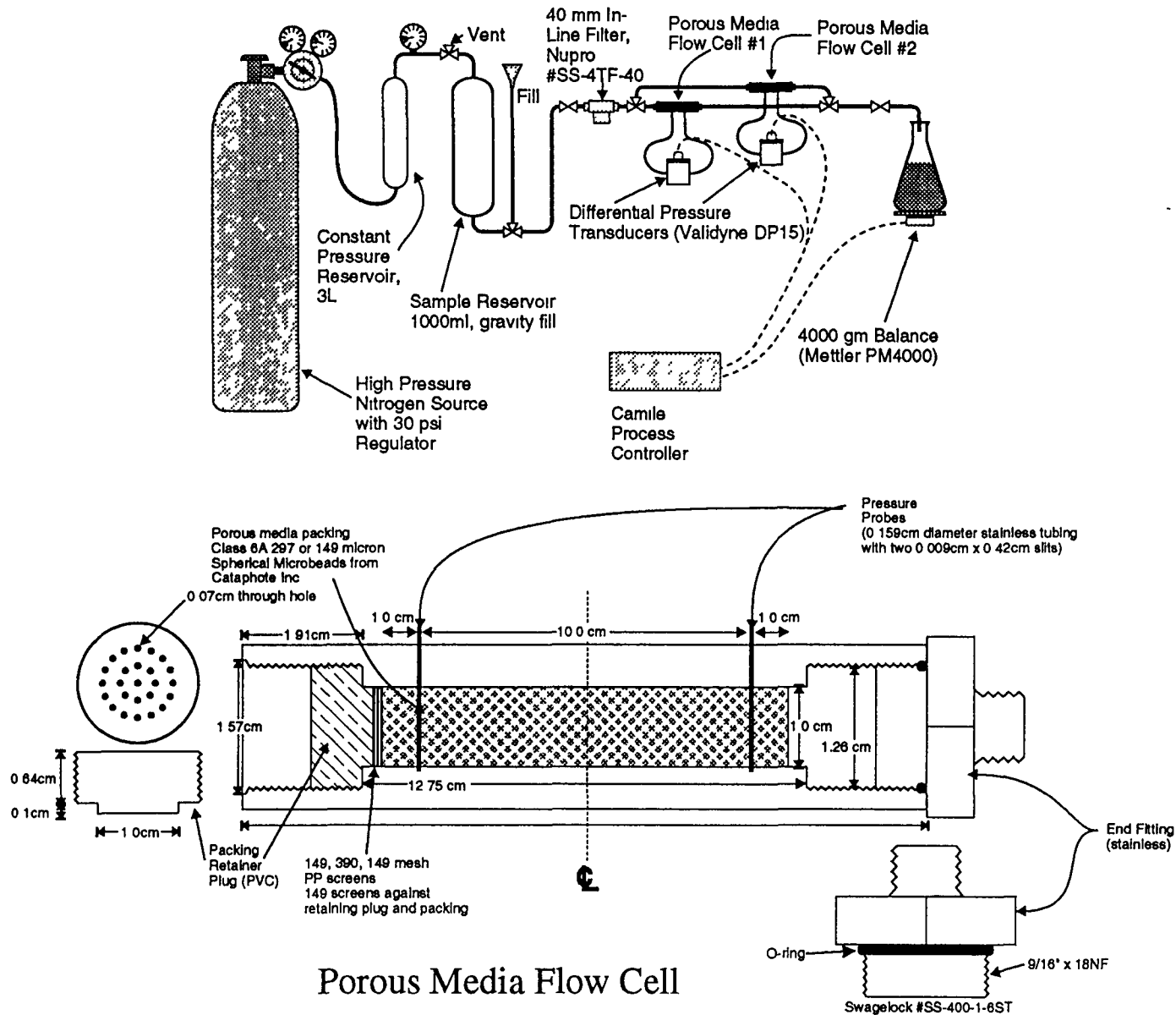
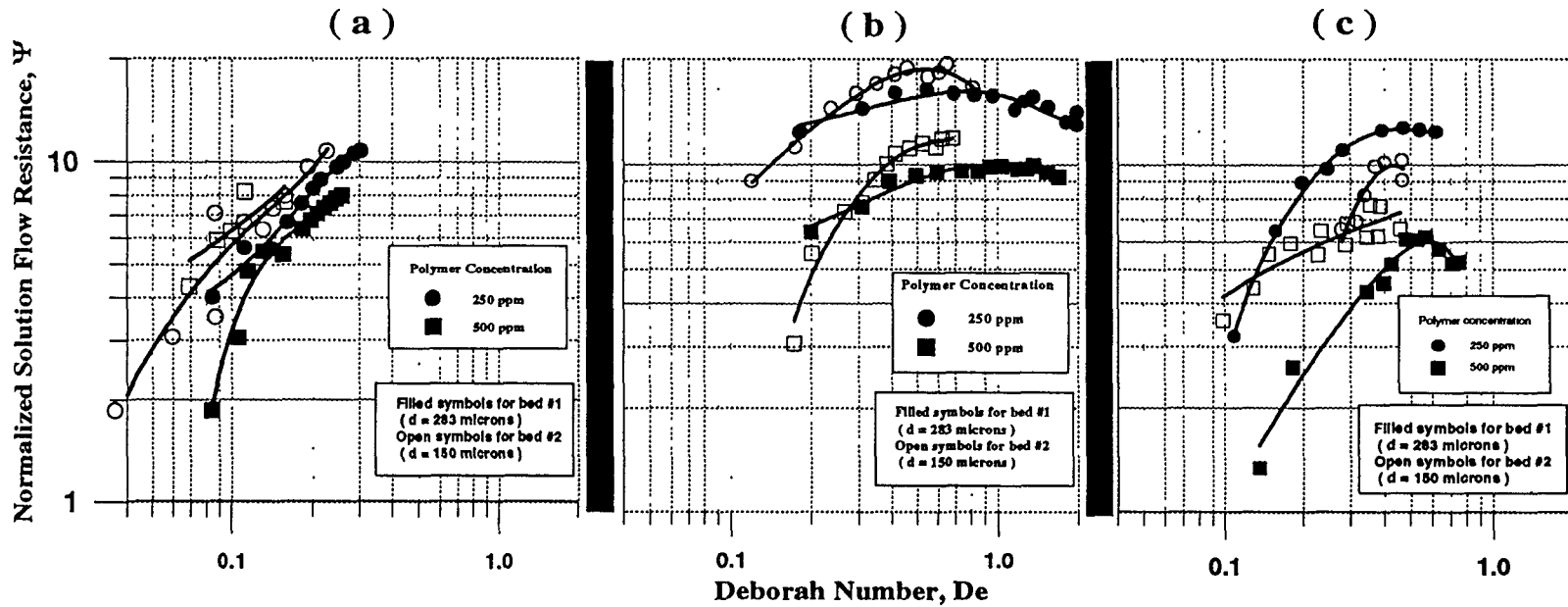


FIGURE 2

FLOW RESISTANCE OF 3-ACRYLAMIDO-3-METHYLBUTANOIC ACID  
 -- ACRYLAMIDE ( MOLE RATIO OF 1 : 9 ) COPOLYMERS AND  
 POLYACRYLAMIDE HOMOPOLYMER SOLUTIONS



NaAMB/AM 10/90 Copolymer in 0.5 M NaCl solvent  
 Weight average molecular weight =  $1.9 \times 10^6$  g / mole  
 Intrinsic viscosity = 4.8 dL / g  
 Polymer Coil Response Time = 0.4 millisec

NaAMB/AM 10/90 Copolymer in 0.5 M NaCl solvent  
 Weight average molecular weight =  $10.9 \times 10^6$  g / mole  
 Intrinsic viscosity = 17.7 dL / g  
 Polymer Coil Response Time = 7.8 millisec

AM Homopolymer in 0.5 M NaCl solvent  
 Weight average molecular weight =  $3.3 \times 10^6$  g / mole  
 Intrinsic viscosity = 7.2 dL / g  
 Polymer Coil Response Time = 1.0 millisec

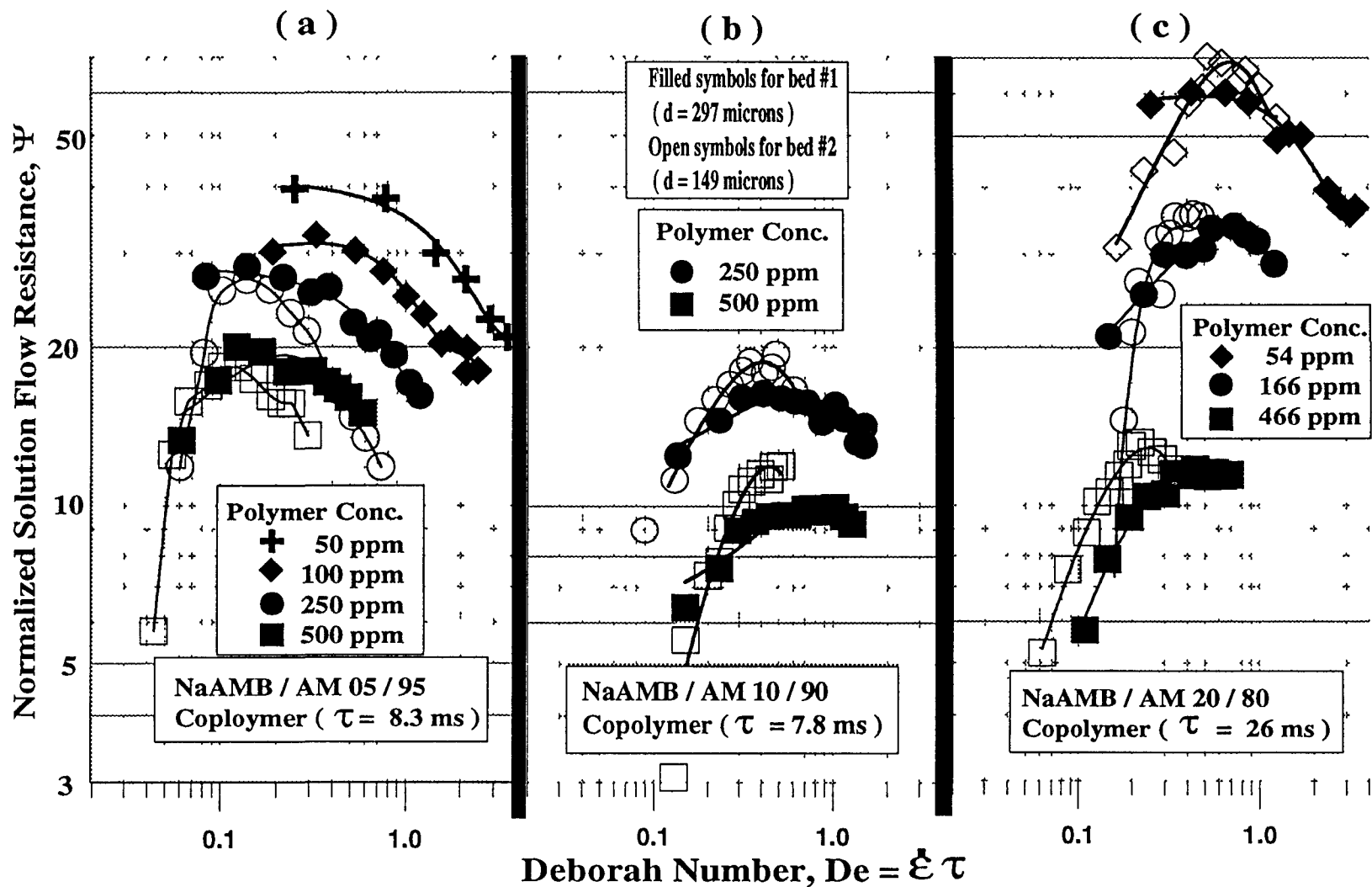


**FIGURE 3 : Durst Plots Showing Flow Resistance of 3-Acrylamido-3-Methylbutanoic Acid--Acrylamide Copolymer Solutions Through Packed Beds at 25 °C**